PHYSICAL REVIEW B VOLUME 34, NUMBER 3 1 AUGUST 1986

# Far-infrared absorption of thin superconducting aluminum films in the pair-breaking and paramagnetic limits

P. J. M. van Bentum and P. Wyder*
*Research Institute for Materials, University of Nijmegen, The Netherlands*
(Received 2 December 1985)

Measurements are presented of the far-infrared absorption of thin superconducting aluminum films in a parallel magnetic field. The results for moderately thick films ($d \approx 10$ nm) are in reasonable agreement with the Abrikosov-Gor'kov theory of pair breaking. The experimental results for ultrathin films ($d \leq 5$ nm) in the paramagnetic limit show that the spectroscopic gap $\Omega_g$ shifts linearly with the magnetic field $H$, according to $\hbar\Omega_g = 2\Delta - 2\mu_0\mu_B H$. This shift of the gap is attributed to a photon-absorption process, where the quasiparticle spin is flipped with respect to the static field. The complex conductivity of a paramagnetically limited film in a parallel magnetic field is calculated, both within the Bardeen-Cooper-Schrieffer framework and using the more general Green's-function formalism with the inclusion of spin-orbit and (magnetic) spin-flip scattering. For the ultrathin Al films we obtain a good quantitative agreement between theory and experiment, assuming a spin-orbit coupling $\hbar/\tau_{SO}\Delta \approx 0.1$ and a reduced value of the imaginary part of the conductivity, probably due to strong electron-phonon coupling effects.

## I. INTRODUCTION

The microscopic BCS theory[1] of superconductivity assumes a simple antiparallel spin pairing. This gives rise to a number of interesting spin-dependent properties: a vanishing (magnetic) spin susceptibility at low temperatures,[2] a Zeeman splitting in the density of states of the quasiparticles for a thin film in a parallel magnetic field,[3] and a first-order transition[4] to the normal state in a parallel magnetic field given by the Clogston value $H_{c,p} = \sqrt{2}\Delta/\mu_0\mu_B$. In spite of the success of the BCS theory, at the earlier times none of the predicted spin-dependent effects were unambiguously confirmed by experiments. Therefore, Bardeen and Schrieffer[5] proposed measurements on aluminum to test the theory and to resolve this problem. Not only is Al a classic example of a weak-coupling superconductor, also its low atomic mass is expected to lead to a negligible spin-orbit coupling. Subsequent experiments on Al have indeed provided convincing evidence for an antiparallel spin pairing of the superconducting ground state. Hammond and Kelly[6] and Fine, Lipsicas, and Strongin[7] showed that the magnetic susceptibility did approach zero by carefully measuring the Knight shift in Al. Critical-field measurements by Strongin and Kammerer[8] and by Meservey, Tedrow, and Schwartz[9] demonstrated the existence of paramagnetic limiting of the critical field $H_c$. The existence of a first-order transition was deduced from a depression of the fluctuation effects at the resistive transition[10] near the critical temperature $T_c$. By far the most convincing evidence was produced in a series of tunneling measurements by Tedrow and Meservey.[11] These experiments proved not only the existence of a Zeeman splitting in the density of states, but gave also detailed information on the strength of the spin-orbit coupling. The Zeeman splitting in the density of states has by now proved to be a valuable tool to study the spin polarization in various ferromagnetic materials.[12]

In the present experiment we have studied in the spin-dependent properties of thin Al films, using far-infrared (FIR) spectroscopic techniques. Our primary aim was to obtain an independent verification of the Zeeman splitting in the density of states. In addition, FIR measurements might provide information on the spin pairing in the BCS ground state by virtue of the fact that the coherent nature of the superconducting state is explicitly involved in electromagnetic absorption. (These coherence factors are, in principle, also involved in the tunneling process, but they cancel again after summation over the various tunnel channels to obtain the total current.[13])

When studying the effect of a parallel magnetic field on a superconductor, one is confronted with two competing effects of the field. For thick films, the Meissner effect is incomplete but the effect on the electron orbits still leads to the well-known pair-breaking effect. Only in the extreme thin limit ($d \leq 5$ nm) is the Meissner effect nearly absent, and the effect of the field on the electron spin becomes dominant. We have measured the far-infrared absorption on thin films in both regimes to be able to discriminate the typical spin-dependent properties. In Sec. III we will present the experimental results for moderately thick films ($d \approx 10$ nm), where the pair-breaking effect of the field still dominates. The absorption spectra will be compared with calculations based on the Abrikosov-Gor'kov (AG) theory.[14] In Sec. IV we will describe the experimental results of the FIR absorption of ultrathin films ($d \approx 4$ nm) in the paramagnetic limit. In Sec. V we will develop a theoretical analysis to calculate the complex conductivity in the paramagnetic regime and compare this with the measurements.

 

## II. EXPERIMENTAL SETUP

Far-infrared spectroscopy, in the hands of Tinkham and collaborators,[15–17] has proved to be a powerful tool to study most of the important properties of superconductivity. Yet, despite the early predictions of spin-dependent properties, no far-infrared experiments have been initiated to tackle this field. This is probably due to the fact that the experimental requirements are rather extreme. First, superconductors with a small spin-orbit interaction such as Al have an energy gap which is located in a rather unaccessible part of the electromagnetic spectrum. The energy gap of bulk Al is 0.34 meV (2.74 $cm^{-1}$ or 82.3 GHz); for thin films, one expects an enhancement of the energy gap up to the order of 0.6 meV ($\approx 4$ $cm^{-1}$ or 120 GHz). This energy is more or less intermediate between the microwave and the far-infrared region. Not only are there no strong radiation sources available for this region, one also has to use spectroscopic techniques that are some sort of a hybrid between optical and single-mode microwave techniques. Second, in order to reach a sufficiently low reduced temperature $T/T_c$, one has to cool the samples to $^3$He temperatures. Third, in order to study paramagnetic effects one must suppress the pair-breaking (diamagnetic) effect of the induced Meissner currents. This can be achieved by using very thin films ($d \leq 5$ nm), carefully aligned (within 0.1°) parallel to the field. The critical field is typically of the order of 5 T.

In our experiment, the thin-film samples were produced by standard evaporation techniques. These films covered the entire surface of a disk-shaped quartz or silicon substrate with a diameter of 9 mm. The electrical and thermal contacts were soldered onto predeposited contacts on the cylindrical sides of the substrates. To prevent oxidation of the films, we covered the thinnest films ($d \approx 3$–4 nm) with an evaporated silicon layer. The samples were mounted inside an oversized cylindrical waveguide system. The lower part of the optical system could be accurately oriented relative to the magnetic field from the top of the cryostat, using a spindle (see Fig. 1). We aligned the film parallel to the field by maximizing the critical-field value. The accuracy of this procedure guaranteed an alignment within 0.05° parallel to the magnetic field.

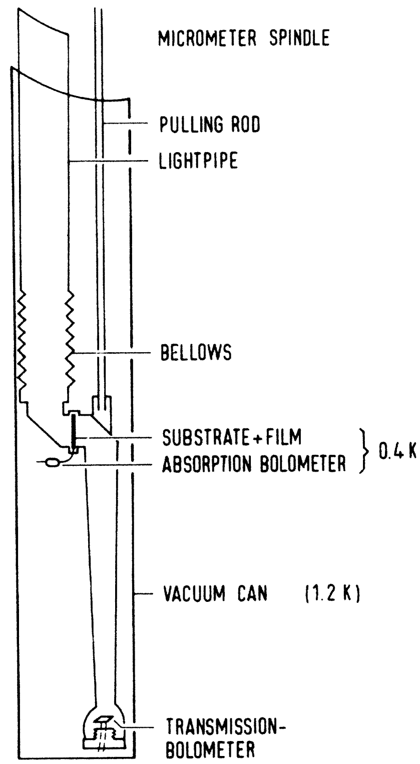


FIG. 1. Lower part of the cryogenic setup. All parts are cooled to 1.2 K, except for the sample and bolometers which are cooled to 0.4 K. The sample holder can be aligned with respect to the direction of the magnetic field by adjusting the setting of a micrometer spindle on top of the cryostat.

The sample was connected to a pumped $^3$He bath with a 0.1-mm gold wire and to a carbon thermometer placed outside the light path. In this setup we could determine the absorption of the film by monitoring the temperature variations in the modulated FIR beam. We used a standard phase-modulated Michelson interferometer, which was optimized for the ultralow-frequency range ($\approx 2$–10 $cm^{-1}$). For more experimental details, we refer to Ref. 18.

In Table I we have summarized the noninfrared properties of the films studied in the present experiment. From the comparison of the experimentally observed critical

TABLE I. General properties of the measured films, where $d$ is the thickness, $R_n$ the normal-state sheet resistance, $T_c$ the critical temperature, $\Omega_g$ the measured spectroscopic energy gap, $H_c$ the experimentally determined value of the parallel critical field at the lowest temperature ($T \approx 0.4$ K), and $H_{c,p}$ the theoretical result for the Clogston field, calculated from the measured gap. In the last column we have indicated the substrate material.

| Film | $d$ (nm) | $R_n$ (Ω) | $T_c$ (K) | $\Omega_g$ ($cm^{-1}$) | $H_c$ (T) | $H_{c,p}$ (T) | Substrate |
|---|---|---|---|---|---|---|---|
| 1 | 27 | 0.2 | 1.21 | | 0.85 | 2.23 | Si |
| 2 | 5 | 560 | 1.51 | 3.45 | 1.84 | 2.78 | Si |
| 3 | 3 | 2100 | 2.03 | 4.45 | 3.80 | 3.74 | Si |
| 4 | 8 | 22 | 1.52 | 3.25 | 1.05 | 2.80 | quartz |
| 5 | 11 | 125 | | 3.41 | | | quartz |
| 6 | 4 | 112 | 1.96 | 4.85 | 3.45 | 3.61 | quartz |
| 7 | 3 | 57 | 2.10 | 5.20 | 3.56 | 3.86 | quartz |
| 8 | 5 | 31 | | 5.20 | | | quartz |

fields and the theoretical Ginzburg-Landau (GL) and Clogston values, we conclude that all films with a thickness less than $\approx 5$ nm are in the paramagnetic limit.

## III. FIR ABSORPTION IN THE PAIR-BREAKING LIMIT

### A. Introduction

The most familiar impact of a magnetic field on a superconducting film is a depairing of the ground state, because it breaks the time-reversal symmetry of the BCS pairing scheme. As shown by Maki and Fulde,[19] all depairing effects can be described in terms of the AG theory, which was originally developed to explain the depairing effects induced by paramagnetic impurities. This theory was extended by Skalski, Betbeder-Matibet, and Weiss[20] and applied to calculate the complex conductivity $\sigma=\sigma_1-i\sigma_2$ in a pair-breaking situation. The predictions of the AG theory have been confirmed in detail by electron tunneling[21] and by FIR-absorption measurements[22] on thin Pb films containing magnetic Gd impurities. Similar films with Mn impurities, however, showed a considerable deviation from theory, characterized by a nonvanishing value of the real part of the conductivity below the gap frequency. Despite the fact that all pair-breaking phenomena have essentially the same effect, it is still of some interest to study the effect of a parallel magnetic field on the complex conductivity. This is related to the fact that the interaction of a Cooper pair with a magnetic impurity is due to a spin exchange rather than to the local magnetic field.[23] Early FIR experiments[17] on Pb films in a parallel magnetic field were in considerable disagreement with the AG theory. This was explained by the authors by assuming a non-negligible perpendicular component of the field, which would create strongly absorbing vortices. Despite the fact that several experiments were undertaken to clarify this point,[24] one must conclude that the question is still not completely settled. More specifically, no other FIR experiments have been performed to investigate the pair-breaking effect of a parallel magnetic field in other (weak-coupling) superconductors.

### B. Experimental results and discussion

Skalski *et al.*[20] showed that the main effect of the magnetic field is a strong reduction of the minimum excitation energy $\Omega_g$ and a less prominent decrease of the order parameter. They also showed that the smearing out of the singularity in the density of states will lead to a much more gradual increase of $\sigma_1$ above the gap frequency.

In the following we will assume that the measured spectroscopic gap at $T=0.4$ K and $H=0$ is to a very good approximation equal to $2\Delta_0$, where $\Delta_0$ denotes the order parameter at $T=0$ and $H=0$. In Fig. 2 we present the absorption spectra $A_s(\omega)/A_n(\omega)$ of the 8-nm-thick Al film 4 for various values of the magnetic field. The data processing included a Fourier transformation of the interferograms, division of the obtained spectrum by the absorption spectrum in the normal state ($H>H_c$), subtraction of a constant background signal, due to radiation leaks and absorption of the substrate, and finally a renormalization to obtain $A_s/A_n=1$ at frequencies far above the gap. This procedure is described in more detail in Ref. 18. Qualitatively, it is clear that we do not find any indication of the presence of vortices, as reported in Ref. 17. Our experimental results of Fig. 2 illustrate clearly that the most important effect of the magnetic field is indeed a depression of the gap and a reduction of the steepness of the absorption edge.

A more quantitative comparison with the AG theory can be provided using the calculations of Skalski *et al.*,[20] valid for films in the dirty limit, i.e., small mean free path $l$. Their final result for the conductivity can be summarized by the equation

$$\frac{\sigma_1(2\omega)}{\sigma_n}=\frac{1}{\omega}\int_{\Omega_g-\omega}^{-\Omega_g+\omega} d\omega'[n(\omega'+\omega)n(\omega'-\omega)+m(\omega'+\omega)m(\omega'-\omega)] \quad (\omega>\Omega_g)\ , \tag{1}$$

where the functions $n$ and $m$ are defined by

$$n(\omega)=\mathrm{Re}\left\{\frac{u}{(u^2-1)^{1/2}}\right\}, \tag{2}$$

$$m(\omega)=\mathrm{Re}\left\{\frac{1}{(u^2-1)^{1/2}}\right\}, \tag{3}$$

and $u$ is the solution of the self-consistent equation

$$u=\frac{\hbar\omega}{\Delta}+i\Gamma\frac{u}{(u^2-1)^{1/2}}\ . \tag{4}$$

The constant $\Gamma$ is the famous pair-breaking parameter. In a parallel magnetic field this $\Gamma$ is simply

$$\Gamma=\tfrac{1}{2}(H/H_c^{\mathrm{GL}})^2\ , \tag{5}$$

where $H_c^{\mathrm{GL}}$ is the Ginzburg-Landau critical field given by

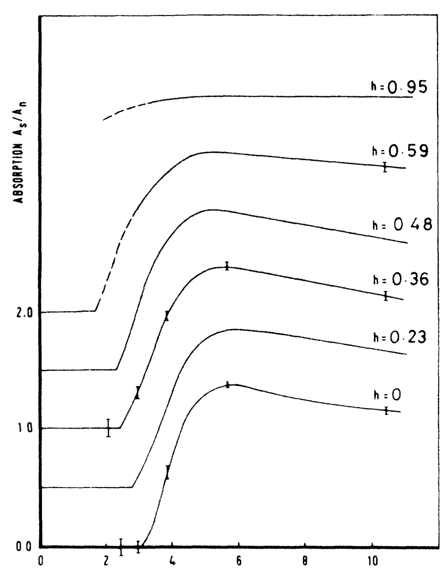


FIG. 2. Absorption $A_s(H)/A_n$ of film 4 ($d=8$ nm) as a function of frequency for different values of the magnetic field $h=H/H_c$.

$$H_c^{\mathrm{GL}} = \frac{\sqrt{24}\lambda H_{c,b}}{d} \tag{6}$$

for a penetration depth $\lambda$, a film thickness $d$, and a bulk critical field $H_{c,b}$. The penetration depth $\lambda$ is a function of temperature $T/T_c$ and mean free path $l$, and can be calculated in a straightforward way from the GL theory.

For an 8-nm-thick film one may assume that $l \approx d$, which gives a critical field $\mu_0 H_{c\parallel}^{\mathrm{GL}}$ of 1.45 T. Experimentally, we find a critical field, extrapolated to $T=0$, of 1.18 T, which is in reasonable agreement.

The paramagnetic Clogston limit is given by

$$H_{c,p} = \frac{\Delta_0}{\sqrt{2}\mu_0\mu_B}\ , \tag{7}$$

which gives a value of 2.42 T for this particular film. indicates that this film is still in the AG pair-breaking limit, although some paramagnetic effects might be visible.

The gap frequency can be determined in a straightforward way from the experimental absorption for small values of the magnetic field. In Fig. 3 we have plotted the experimental gap values, which were determined by extrapolating the linear part of the absorption curve to zero absorption. This procedure might give a slight overestimate of $\Omega_g$, since it ignores a possible small tail near the absorption edge. An accurate determination of the gap value was possible only for the lowest values of the field, because of the very low power output of the interferometer below 2 cm.$^{-1}$ The solid curve in Fig. 3 represents the theoretical calculation by Skalski *et al.*[20] of the gap as a function of the depairing magnetic field $H/H_c$, where $H_c$ is the measured critical field. As can be seen from the figures, we find a reasonable agreement between between experiment and theory. Using the conductivity as calculated according to Eq. (1), we can make a further, more quantitative comparison with the AG theory. The absorption of a thin film with conductivity $\sigma=\sigma_1-i\sigma_2$ on the rear side of a wedge-shaped substrate with refractive index $n$ is given by[18]

$$\frac{A_s}{A_n} = \frac{4nz\sigma_1/\sigma_n}{z^2\sigma_1^2/\sigma_n^2 + z^2\sigma_2^2/\sigma_n^2 + (n^2+3)z\sigma_1/\sigma_n + 2n^2 + 2}\ , \tag{8}$$

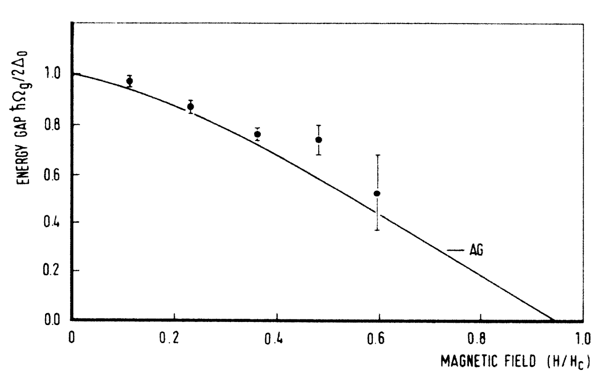


FIG. 3. Spectroscopic gap $\Omega_g$ as a function of the parallel magnetic field for film 4 (dots). The solid line indicates the result of the AG pair-breaking theory.

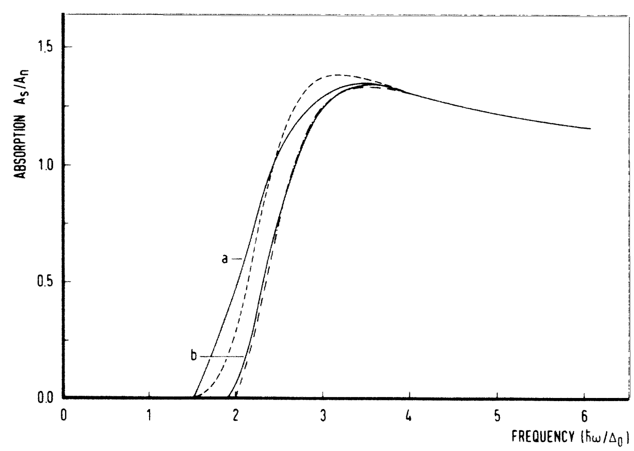


FIG. 4. Absorption $A_s(H)/A_n$ of film 4 for $H/H_c=0.36$ and $T/T_c=0.2$ compared with a theoretical calculation using $\sigma^{\mathrm{AG}}$ ($\Gamma=0.06$), $R_n=6\ \Omega$, and $n=2.1$ (dashed line). For comparison, we have plotted the zero-field absorption (curve $b$), together with a weak-coupling calculation using $\sigma^{\mathrm{MB}}$, $R_n=6\ \Omega$, and $n=2.1$ (dashed-dotted line).

where $z=377/R_n$ is the vacuum impedance divided by the normal-state sheet resistance of the film.

We find an excellent agreement between the experimental absorption at $H=0$ (solid curve $b$ in Fig. 4) and a theoretical calculation, using the weak-coupling Mattis-Bardeen (MB) conductivity and treating the constant $z$ as a fit parameter (dashed-dotted line in Fig. 4). In principle, $z$ can be determined from the measured value of $R_n$. Unfortunately, dc measurements do not give reliable values for the film resistivity due to grain boundaries, etc. For more details, see Ref. 18. For $H/H_c=0.36$ we have calculated the absorption using Eqs. (1) and (8) with the same value for $z$. This result is indicated in Fig. 4 with a dashed line, together with the experimental result (solid curve $a$).

The general agreement between the experimental curves and the AG-Skalski theory is reasonable. However, there are some distinct deviations. The most obvious difference is that the onset of the absorption edge is more linear than predicted from theory. The origin of this effect is not clear, although one might think of an additional spin-orbit scattering, which does not reduce the order parameter, but which does smear out the singularity in the BCS density of states. We also may expect some spin paramagnetic effects for this particular film, since $\mu_0\mu_B H/\Delta$ is not completely negligible. For example, at $H/H_c=0.36$ we find $\mu_0\mu_B H/\Delta \approx 0.10$, which shows that paramagnetic effects might play a role.

## IV. FIR ABSORPTION OF ULTRATHIN AL FILMS IN THE PARAMAGNETIC LIMIT

In this section we will examine the spin paramagnetic effect on the FIR absorption in more detail. We will first present the experimental results for some ultrathin films. As calculations of the field-dependent complex conductivity of a film in the paramagnetic limit have not appeared in the literature, we will summarize the concepts relevant for a theory of the complex conductivity of a superconductor with a Zeeman-split density of states within the framework of the BCS theory. In the last part of this section we will also allow for spin-orbit coupling and (magnetic) spin-flip scattering. In particular, we will concentrate on the possibility of photon-induced spin-flip excitations. The agreement between theory and experiment will be discussed.

The absorption measurements were performed with the same setup as described in Sec. III. Because of the better impedance matching of the ultrathin films to the vacuum impedance, we obtain a larger absorption signal. A second advantage is the fact that the gap for these films is shifted to a higher frequency, which allows us to measure the field-dependent effects for larger values of the parallel magnetic field.

In an attempt to determine if a first-order phase transition takes place at $H_c$, we measured the microwave absorption of film 6 as a function of the field. If the transition is of first order, we expect an almost zero absorption below $H_c$ and a sudden discontinuous jump to the normal-state absorption at the Clogston field. In Fig. 5 we have plotted the microwave absorption of film 6 as a function of the field. The frequency of the radiation was 38 GHz, equivalent with $\hbar\omega = 0.25\Omega_g$. This curve appears to be in reasonable agreement with theoretical predictions. Below $H_c$, the absorption rises slowly as a function of the field, which indicates that the number of quasiparticles is enhanced by the (small) pair-breaking effect of the field. What is interesting, however, is the sharp kink in the curve at $H \approx H_c$. This structure is much sharper than the width commonly found for the resistive transition of these wide and more or less granular films. The AG theory (dashed line) also gives a sharp transition at $H_c$, but one usually finds that this transition is significantly rounded due to fluctuations of the order parameter above $H_c$. The fact that no such rounding off is found might indicate that there is a first-order transition at the Clogston field.

In Fig. 6 we present the FIR-absorption spectra of film 6, which had a normal-state resistance of 110 Ω. This resistance is very close to the optimum value for an ideal matching to the vacuum impedance for a film on a quartz substrate. The agreement with the BCS theory of the $H=0$ curve has already been discussed in Ref. 18. With an increasing magnitude of the parallel magnetic field, we find the following qualitative changes in the absorption spectrum: An additional absorption below the gap increases in magnitude with increasing field. The onset of this shoulder shifts to a lower frequency approximately linearly with the field.

In other words, we find a spectroscopic gap which decreases linearly with $H$. A second characteristic of the absorption spectrum is the presence of a distinct kink near the zero-field gap. Only for very high values of the field has this structure disappeared. For some films we also observed a less distinct structure above the gap, which shifted to higher frequencies with increasing field. However, this effect was not very reproducible and could not clearly be discriminated from the noise. The position of the characteristic structures in the absorption spectra is studied in more detail in Fig. 7, where we have plotted the spectroscopic gap value and the position of the kink around $2\Delta$ for film 6. The position of the kinks were determined by extrapolating the linear parts of the absorption curves.

In Fig. 7 we have plotted the energy shift of the spectroscopic gap $\hbar\Omega_g$ from the measured value of the kink at $2\Delta$ as a function of the magnetic field. The solid lines in Fig. 7 represent the simple relations $\hbar\omega = 2\Delta$ and

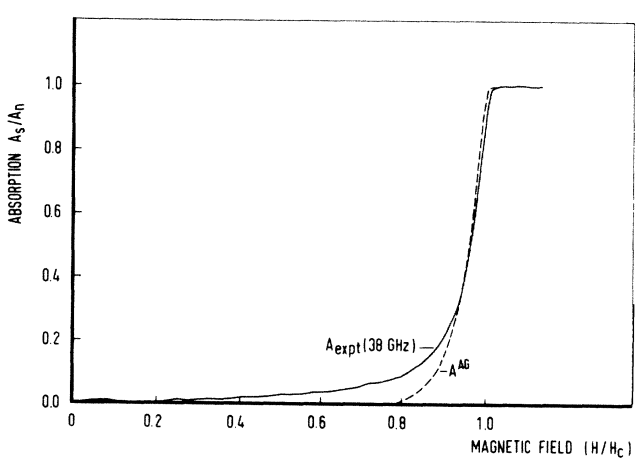


FIG. 5. Microwave absorption of film 6 ($\hbar\omega \approx \Delta_0/2$) as a function of the parallel magnetic field (solid curve), compared with a theoretical calculation based on the Abrikosov-Gor'kov (AG) theory (dashed line).

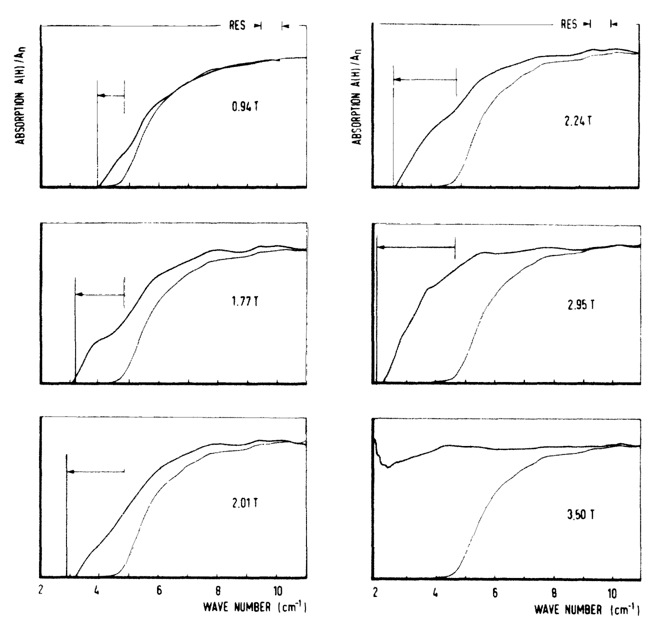


FIG. 6. Absorption $A_s(H)/A_n$ of film 6 ($d=4$ nm) as a function of frequency for different values of the parallel magnetic field, as indicated. The arrows indicate the theoretically expected shift of the energy gap ($\Omega_g = 2\Delta - 2\mu_0\mu_B H$). The measured absorption at $H=0$ is indicated for reference (lower curve in every plot).

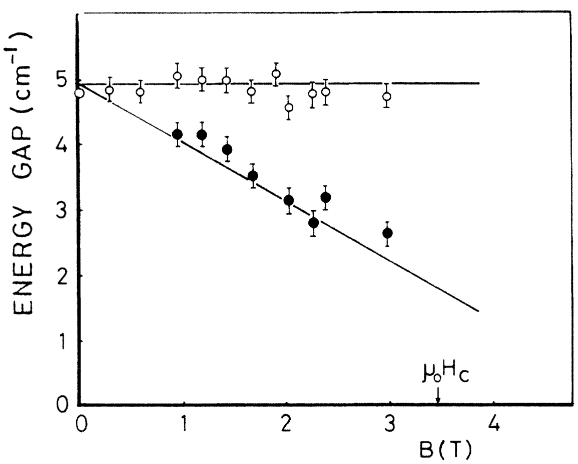


FIG. 7. Spectroscopic gap (●) and position of the kink in the absorption (○) as a function of the parallel magnetic field for film 6. The solid lines indicate the theoretically expected relation $\hbar\omega=2\Delta$ and $\hbar\omega=2\Delta-2\mu_0\mu_B H$.

$\hbar\omega=2\Delta-2\mu_0\mu_B H$. The good general agreement suggests that the additional absorption is related with the paramagnetic shift in energy of the singularity in the spin-dependent density of states for the quasiparticles.

## V. THEORY

### A. Electromagnetic response in the paramagnetic limit

In this section we will calculate the complex conductivity of a superconducting film in the presence of a parallel magnetic field and in the paramagnetic limit. Mattis and Bardeen[25] and Bardeen and Schrieffer[5] have evaluated the conductivity in the extreme anomalous limit, where the penetration depth of the field is small compared to the superconducting coherence length. Their approach is also valid in the dirty limit, where the mean free path is smaller than the coherence length. We will first summarize the MB results, and subsequently develop an equivalent scheme to calculate the conductivity in the presence of a parallel field.

In the paramagnetic limit, where we neglect the effect of the field on the electron orbits, the time-reversal symmetry of the Cooper pairing is not broken and we can describe the electromagnetic properties entirely within the framework of the BCS theory.

In order to calculate the transition probabilities between the energy levels $E$ and $E+\hbar\omega$, we have to consider the coherent nature of excitations from a state $(k,s)$ to $(k',s')$ and from $(-k,-s)$ to $(-k',-s')$. We use the notation $s$ for the spin to avoid confusion with the conductivity $\sigma$. The evaluation of the transition probabilities can be done most easily by introducing the so-called coherence factors

$$F(E,E',\Delta)=F(E,E+\hbar\omega,\Delta)\ .$$

These coherence factors take into account that the matrix elements governing these excitations must be added with a proper phase factor and squared before summing over all $k$ states. As shown by Bardeen and Schrieffer,[5] these coherence factors do not depend on the interaction of the external perturbation with the spin, but are solely determined by the even or odd nature of the perturbation under time reversal of the electronic states. For electromagnetic absorption the so-called "case-II" coherence factors are appropriate: $F=(u_k u_{k'}+v_k v_{k'})^2$ in the case of scattering of quasiparticles and $F=(v_k u_{k'}-u_k v_{k'})^2$ in the case of creation or annihilation of quasiparticles.

If one adopts a sign convention such that the excitation energy $E_k$ and the kinetic energy $\xi_k$ have the same sign, the coherence factor for both scattering and creation and/or annihilation is given by a single expression:

$$F(E,E',\Delta)=\frac{1}{2}\left[1+\frac{\Delta^2}{E_k E_{k'}}\right]\ , \tag{9}$$

where $E_k=(\Delta^2+\xi_k^2)^{1/2}$.

The net probability for a transition from $E$ to $E+\hbar\omega$ is then proportional to

$$\alpha_s \approx \int_{-\infty}^{\infty}\{F(E,E+\hbar\omega\,\Delta)N_s(E)N_s(E+\hbar\omega)\times[f(E)-f(E+\hbar\omega)]\}dE\ , \tag{10}$$

where $N_s$ denotes the superconductive density of states for the quasiparticles, and $f(E)$ is the density of occupied quasiparticle states at energy $E$.

In the extreme anomalous limit this leads to the famous Mattis-Bardeen expressions for the complex conductivity[25]:

$$\frac{\sigma_1}{\sigma_n}=\frac{2}{\hbar\omega}\int_{\Delta}^{\infty}\{F(E,E+\hbar\omega,\Delta)N_s(E)N_s(E+\hbar\omega)[f(E)-f(E+\hbar\omega)]\}dE + \frac{1}{\hbar\omega}\int_{\Delta-\hbar\omega}^{-\Delta}\{F(E,E+\hbar\omega,\Delta)N(E)N(E+\hbar\omega)[1-2f(E+\hbar\omega)]\}dE\ , \tag{11}$$

where the first term represents the contribution connected with quasiparticle scattering and the second term gives the pair-breaking contribution. $\sigma_2$ follows directly using the Kramers-Kronig relations[26] and the Tinkham-Ferrell sum rule:[27]

$$\frac{\sigma_2}{\sigma_n}=\frac{2}{\pi\omega}\int_{0^+}^{\infty}\frac{\sigma_n-\sigma_1(\omega')}{\sigma_n}d\omega'-2\frac{\omega}{\pi}\int_{0^+}^{\infty}\frac{\sigma_1(\omega')}{(\omega')^2-\omega^2}d\omega'\ . \tag{12}$$

In the absence of spin-orbit or spin-flip scattering, we may write the Hamiltonian of a superconductor in a magnetic field as[28]

$$H=\sum_{k,s}\xi_k a^{\dagger}_{k,s}a^{\dagger}_{-k,-s}a_{-k',-s'}a_{k',s'} -2\mu_0\mu_B\sum_{k,s}a^{\dagger}_{k,s}a_{k,s}\mathbf{s}\cdot\mathbf{H}\ , \quad (13)$$

where $\xi_k$ denotes the orbital energy of an electron in a state with wave number $k$.

In an antiparallel pairing scheme, the field does not affect the superconducting ground state, and we may rewrite this Hamiltonian in terms of the elementary excitations:

$$H=\mu N_{0p}+E_g+\sum_k E_k\gamma_k^{\dagger}\gamma k-2\sum_i \mu_0\mu_B s_i H\ , \quad (14)$$

where the summation over $i$ runs over all occupied quasiparticle states, $\mu$ is the chemical potential, $N_0$ the number operator, $E_g$ the energy of the superconducting ground state, $\gamma_k$ are the well-known Bogoliubov operators describing the elementary excitations from the ground state, and $s_i$ denotes the expectation value of the quasiparticle spin along the field direction.

If we take the excitation energies relative to the Fermi energy ($\mu=0$), then both electronlike and holelike quasiparticles have an excitation energy given by

$$\begin{aligned} E(k,s)&=E_k-2\mu_0\mu_B sH\\ &=E_k\pm\mu_0\mu_B H=(\Delta^2+\xi_k^2)^{1/2}\pm\mu_0\mu_B H\ , \end{aligned} \quad (15)$$

where the $\pm$ sign depends on the direction of the quasiparticle spin. The simplest excitation process that involves the absorption of a photon is described by the creation of an electronlike and a holelike quasiparticle with the simultaneous annihilation of a Cooper pair. The energy of a Cooper pair does not depend on $H$, due to the antiparallel spin pairing. The total excitation energy of this process is

$$\hbar\omega=E_k+E_{k'}-2(s+s')\mu_0\mu_B H\ . \quad (16)$$

If the spin is conserved during the pair-breaking process, then $s=-s'$ and the excitation energy does not depend on the value of the field.

Let us further assume that the intrinsic spin-flip scattering time (due to magnetic impurities or due to the static field) is long compared to the Cooper-pair lifetime, which is of order $\hbar/\Delta$. Then we expect that the spin polarization of the thermally excited quasiparticles is zero, and the occupation numbers $f_{\uparrow}(E)$ and $f_{\downarrow}(E)$, respectively, of the spin-up and spin-down quasiparticles are equal, but shifted in energy:

$$\begin{aligned} f_{\uparrow}(E)&=\frac{1}{1+e^{(E-\mu_0\mu_B H)/kT}}\ ,\\ f_{\downarrow}(E)&=\frac{1}{1+e^{(E+\mu_0\mu_B H)/kT}}\ . \end{aligned} \quad (17)$$

The densities of states for spin-up and spin-down quasiparticles can be calculated using the relation

$$\frac{N(E)}{N(0)}=\frac{d\xi}{dE}\ . \quad (18)$$

In the semiconductor sign convention, we obtain

$$\begin{aligned} N_{\uparrow}(E)&=\tfrac{1}{2}N(0)\frac{|E-\mu_0\mu_B H|}{[(E-\mu_0\mu_B H)^2-\Delta^2]^{1/2}}\ ,\\ N_{\downarrow}(E)&=\tfrac{1}{2}N(0)\frac{|E+\mu_0\mu_B H|}{[(E+\mu_0\mu_B H)^2-\Delta^2]^{1/2}}\ . \end{aligned} \quad (19)$$

The coherence factors follow immediately, using Eq. (9):

$$\begin{aligned} F_{\uparrow\uparrow}&=\frac{1}{2}\left[1+\frac{\Delta^2}{(E-\mu_0\mu_B H)(E'-\mu_0\mu_B H)}\right]\ ,\\ F_{\downarrow\downarrow}&=\frac{1}{2}\left[1+\frac{\Delta^2}{(E+\mu_0\mu_B H)(E'+\mu_0\mu_B H)}\right]\ . \end{aligned} \quad (20)$$

With these ingredients, we can now calculate the conductivity similarly as in Eq. (11), but now the integration must be done separately for the two spin directions. Substituting the relevant expressions for $E$, $f(E)$, $F(E,E+\hbar\omega,\Delta)$, and $N(E)$ in Eq. (11) and changing variables, we find that, when the total spin is conserved in the absorption process, the complex conductivity is independent of the field and $\sigma=\sigma^{\mathrm{MB}}$.

With similar arguments it can be shown that also no changes occur in the tunnel current between two paramagnetically limited superconductors in an magnetic field, by virtue of the fact that the spin of a quasiparticle is not flipped in the tunneling process. In a electromagnetic field, however, there is a finite probability of a spin flip. If one assumes that only the $H$ component of the electromagnetic field perpendicular to the static field flips the spin, then an upper limit of 0.5 is obtained for the spin-flip probability in unpolarized light, directed along the axis normal to the film. This spin-flip probability has a remarkable effect on the absorption spectrum. This can be shown schematically, using the semiconductor model, which pictures the pair-breaking process as a one-particle scattering from a state below the Fermi energy to a state above the Fermi energy. Let us look, for example, at a transition from a spin-up state to a spin-down state in Fig. 8. The minimum excitation energy for this spin-flip scattering process is given by

$$\hbar\Omega_g=2\Delta-2\mu_0\mu_B H\ . \quad (21)$$

We come to the rather surprising conclusion that, although the field has no influence on the superconducting ground state, it does have a strong effect on the spectroscopic gap, which shifts linearly with the field strength. To our knowledge, this effect is not described in the literature. Using the semiconductor model, one can easily predict the qualitative charactersitics of the absorption spectrum. In addition to the spin-flip absorption branch starting at $2\Delta-2\mu_0\mu_B H$, mentioned above, we expect a second branch to appear at $2\Delta$. This branch corresponds to the two transition channels where the total spin is conserved. Finally, a third branch is possible, starting at $2\Delta+2\mu_0\mu_B H$, which corresponds to a spin flip antiparallel to the field. If $T\neq0$ we may even expect a fourth

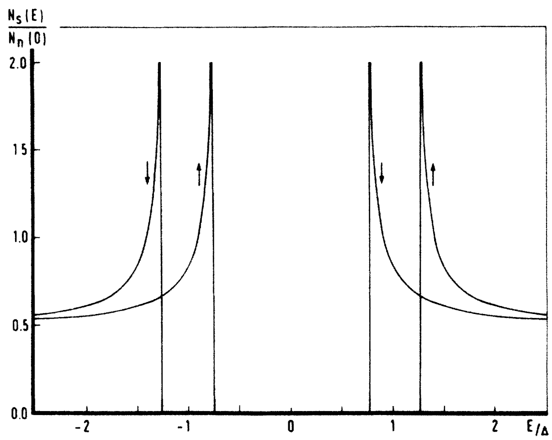


FIG. 8. The Zeeman-split density of states for spin-up and spin-down quasiparticles in the semiconductor model, for a magnetic field $\mu_0\mu_B H=\Delta/4$.

characteristic structure in the absorption spectrum at $\hbar\omega=2\mu_0\mu_B H$, corresponding to a quasiparticle scattering from a spin-down state to a spin-up state.

In the following we will examine these additional spin-flip transition processes in more detail and calculate the total conductivity, which determines the electromagnetic properties of the sample.

In addition to the coherence factors $F_{\uparrow\uparrow}$ and $F_{\downarrow\downarrow}$, we must now also consider the coherent nature of all the possible excitations which involve a spin flip:

$$F_{\uparrow\downarrow}=\frac{1}{2}\left[1+\frac{\Delta^2}{(E-\mu_0\mu_B H)(E'+\mu_0\mu_B H)}\right],$$
$$F_{\downarrow\uparrow}=\frac{1}{2}\left[1+\frac{\Delta^2}{(E+\mu_0\mu_B H)(E'-\mu_0\mu_B H)}\right]. \quad (22)$$

The net transition rate between $E$ and $E+\hbar\omega$ is proportional to $|A_{kk'}A_{ss'}|^2$, the squared matrix element connecting the initial state with energy $E(k,s)$ and the final state with $E'=E(k',s')$. $|A_{ss'}|^2$ denotes the probability that the spin of the excited particle is changed from $s$ to $s'$ by the interaction with a photon.

To get the net rate of absorption of energy, one must take the difference between direct absorption and emission, and sum over all initial states. We finally obtain, for the scattering of quasiparticles,

$$\frac{\sigma_1}{\sigma_n}=\sum_{s,s'}\frac{1}{\hbar\omega}\int dE\,|A_{ss'}|^2F_{ss'}(E,E+\hbar\omega,\Delta)N_s(E)N_{s'}(E+\hbar\omega)[f_s(E)-f_{s'}(E+\hbar\omega)]\,. \quad (23)$$

For the creation of quasiparticles (pair breaking) we find, by generalizing the Mattis-Bardeen equation,

$$\frac{\sigma_1}{\sigma_n}=\sum_{s,s}\frac{1}{\hbar\omega}\int dE\,|A_{ss'}|^2F_{ss'}(E,E+\hbar\omega,\Delta)N_s(E)N_{s'}(E+\hbar\omega)[1-2f_s(E+\hbar\omega)]\,. \quad (24)$$

In practical cases we will always measure the absorption at the lowest achievable temperature, where the occupation numbers of quasiparticles are negligible and we only have to consider the pair-breaking term.

In Fig. 9 we have calculated the low-frequency ($\hbar\omega<2\Delta$) part of the conductivity; at these low frequencies, only quasiparticle scattering takes place, and the integral (24) is zero. The total conductivity is found by summing over the four transition channels. All transitions give a contribution to the conductivity which monotonically decreases with frequency, except for the contribution related with the scattering of a spin-down particle to a spin-up state. This spin-flip transition gives rise to a singularity at $\hbar\omega=2\mu_0\mu_B H$. This peak can be observed only at moderately high temperatures, where the number of quasiparticles is large. In Fig. 10 we have plotted the high-frequency ($\hbar\omega\geq 2\Delta$) conductivity at $T=0$, which is determined by pair breaking only, and the integral (23) is zero. In these calculations we have assumed a spin-flip probability of 0.5. The most interesting result is the fact that $\sigma_{\uparrow\downarrow}$ is the most prominent contribution to the total conductivity. For a spin-flip probability of 0.5 we find that the $\sigma_{\uparrow\downarrow}$ branch goes through a maximum before reaching the high-frequency limit of 0.25. This is a consequence of the fact that the Tinkham-Ferrell sum

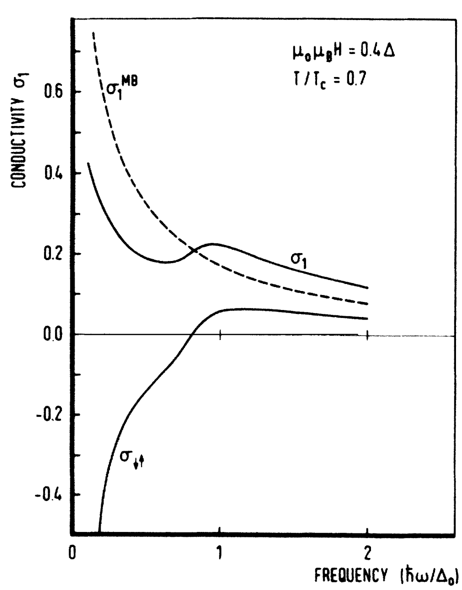


FIG. 9. Low-frequency part of the real conductivity $\sigma_1(\omega)$ as a function of frequency for a superconductor in the paramagnetic limit ($\mu_0\mu_B H=0.4\Delta$, $T/T_c=0.7$). (a) Spin-flip contribution $\sigma_{\uparrow\downarrow}$. (b) Total conductivity. Dashed line: real part of the conductivity at $H=0$, $T/T_c=0.7$.

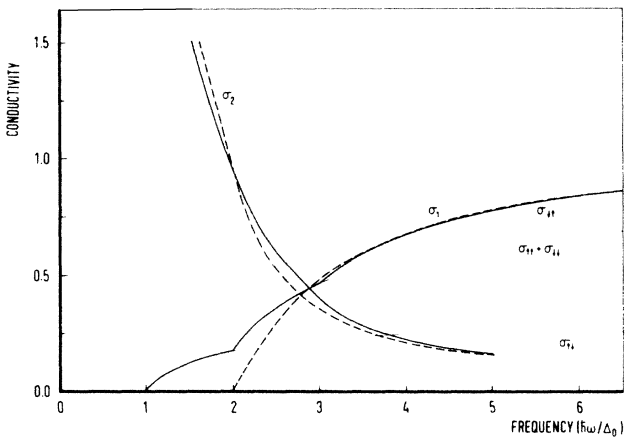


FIG. 10. Complex conductivity of a superconductor in the paramagnetic limit, assuming a spin-flip probability of 0.5 and $\mu_0\mu_B H = \Delta/2$. The separate contributions to the real part of the conductivity $\sigma_1$ are indicated. The imaginary part of the conductivity was calculated using the Kramers-Kronig relations. The dashed lines represent the weak-coupling Mattis-Bardeen results for $H = 0$.

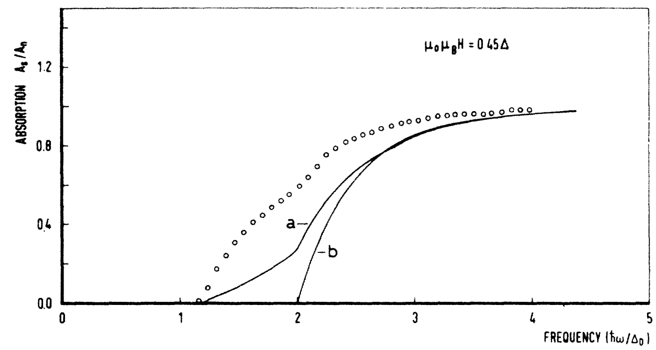


FIG. 11. Comparison of the experimental absorption $A_s/A_n$ (○) as a function of frequency for film 6 ($\mu_0\mu_B H \approx 0.45\Delta$), with theory (curve $a$), using $\sigma_1$ as shown in Fig. 10. Curve $b$ represents the zero-field absorption, which is indicated for reference.

rule only applies to the total transition probability, but is not valid for the individual spin-dependent channels. The $\sigma_2$ curve in Fig. 10 was calculated using the Kramers-Kronig relations. With these results for the complex conductivity, we have all the ingredients we need to calculate the absorption, using Eq. (8).

In Fig. 11 we have compared the experimental result for the absorption in a field $H = 0.45\Delta/\mu_0\mu_B$ (○) with a theoretical calculation according to Eqs. (23), (24), and (8) (curve $a$). For this calculation we used the values $R_n = 110\ \Omega$ and $n = 2.1$. The theoretical absorption for zero field (curve $b$) was added for reference. A major discrepancy between theory and experiment is the large value of the spin-flip absorption.

This unexpectedly high value of the absorption could indicate a larger spin-flip probability than assumed in the theory. However, it seems unlikely that the spin-flip probability could be larger than 0.5 for an unpolarized FIR beam. For the experimental setup we may expect the radiation to be incident on the film within a cone with a top angle of 20° normal to the film. For this situation, we find an electromagnetic $H$ component perpendicular to the static field which is slightly larger than 0.5, but it is not large enough to explain the relative magnitude of the low-energy branch. A possible anomalously low value of the imaginary part of the conductivity $\sigma_2$ (for example, due to pair breaking) might explain the absorption curves at weak magnetic fields, but it cannot explain the large absorption observed at higher fields. One expects from the calculations of Engler and Fulde[29] that for a small pair-breaking effect of the magnetic field the density of states for spin-up and spin-down quasiparticles is still displaced by $\mu_0\mu_B H$, but also the field smears out the singularity at $E = \Delta$. This results in a broadening of the characteristic structures in the absorption spectrum, rather than an increase in magnitude. However, the presence of spin-orbit scattering may also affect the electromagnetic properties.

### B. Spin-orbit coupling

In this section we will evaluate the effect of spin-orbit coupling and of (magnetic) spin-flip scattering on the density of states and calculate the complex conductivity for that case. In the presence of a spin-flip mechanism the BCS approximation of a simple $s = 0$ and $k = 0$ pairing is no longer valid and the superconducting ground state results from a more general pairing between time-reversed electron states. With spin-orbit scattering we will denote all nonmagnetic interactions that may flip the quasiparticle spin. The quasiparticle density of staes of a superconductor in the presence of spin-orbit and spin-flip scattering can be calculated using the more general Green's-function formalism as developed by Abrikosov and Gor'kov,[30] Nambu,[31] and Keller and Benda.[32]

The density of states of quasiparticles with a specific spin direction is obtained from the one-particle Green's function $G_s(\mathbf{k},\omega)$.[29,33]

$$N_s(\omega) = -\frac{1}{2\pi}\mathrm{sgn}(\omega)\mathrm{Im}\left[\int \frac{1}{(2\pi)^3} d^3k\, G_s(\mathbf{k},\omega)\right] . \quad (25)$$

$G_s(\mathbf{k},\omega)$ is generally of the form

$$G_s(\mathbf{k},\omega) = \frac{\tilde{\omega}_s + \xi_k}{\tilde{\omega}_s^2 - \xi_k^2 - \tilde{\Delta}_s^2} . \quad (26)$$

Bruno and Schwartz[33] have solved the generalized function $\tilde{\omega}_s$ and $\tilde{\Delta}_s$ for a scattering potential with, respectively, a spin-independent, a spin-orbit, and a spin-flip part:

$$V(\mathbf{k},\mathbf{k}') + \frac{iV_{\mathrm{SO}}}{k_F^2}(\mathbf{k}\times\mathbf{k}')\cdot\mathbf{s} + w_{\mathrm{SF}}(k,k')\mathbf{s}\cdot\mathbf{S}_i . \quad (27)$$

A compact formulation can be given in terms of the scattering times:

$$\frac{\hbar}{\tau_{\rm SO}} = \tfrac{1}{3} n_1 N(0) \int d\Omega' \, | V_{\rm SO} |^2 \sin^2\theta \, ,$$
$$\frac{\hbar}{\tau_{\rm SF}} = n_2 N(0) S(S+1) \int d\Omega' \, | w_{\rm SF}(\mathbf{k},\mathbf{k}') |^2 \, , \quad |\mathbf{k}'| = k_F \tag{28}$$

where $N(0)$ is the electron density of states of one spin direction on the Fermi surface and $n_1$ and $n_2$ are the densities of nonmagnetic and magnetic scattering centers.

The final result for the density of states can now be written as[29,33]

$$n_\pm = n_{\uparrow,\downarrow}(E) = N(0)\,\mathrm{Re}\left[\frac{u_\pm}{(u_\pm^2-1)^{1/2}}\right] , \tag{29}$$

where the functions $u_s = u_\pm$ are solutions of the coupled equations

$$\frac{E \mp \mu_0\mu_B H}{\Delta} = u_\pm + \frac{\hbar}{\tau_{\rm SO}\Delta}\frac{u_\pm - u_\mp}{(1-u_\pm^2)^{1/2}} - \frac{\hbar}{3\tau_{\rm SF}\Delta}\left[\frac{u_\pm}{(1-u_\pm^2)^{1/2}} - \frac{u_\pm + u_\mp}{(1-u_\mp^2)^{1/2}}\right] . \tag{30}$$

When both $\tau_{\rm SO}$ and $\tau_{\rm SF}$ go to infinity, $u_s$ is real and Eq. (29) is identical to the Zeeman-split BCS expression for the density of states of Eq. (19).

We have numerically solved the coupled equations (30), using an iterative procedure. Figure 12 shows some representative results for the densities of states for $\tau_{\rm SF} = \infty$, $\mu_0\mu_B H = 0.5\Delta$, and for relatively low spin-orbit-scattering rates: (a) $\tau_{\rm SO} = \infty$, (b) $\hbar/\tau_{\rm SO}\Delta = 0.1$, and (c) $\hbar/\tau_{\rm SO}\Delta = 0.2$. This calculation of the densities of states reproduces the results of Refs. 29 and 33 and shows that the effect of a small spin-orbit coupling can be described with a simple mixing of the quasiparticle states for both spin directions.

The most interesting effect of the spin-orbit coupling is a shift of some of the spin-up states to lower energies. In addition, we find that the singularity in the density of spin-up states at $E = \Delta + \mu_0\mu_B H$ is strongly smeared out. The density of states for spin-down quasiparticles is less affected, the most important effect being a shift of the onset to an energy slightly higher than $\Delta - \mu_0\mu_B H$.

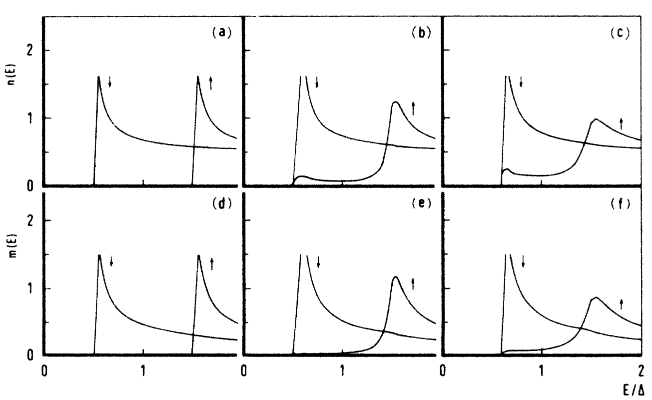


FIG. 12. Zeeman-split density of states $n(E)$ for spin-up and spin-down quasiparticles for a film in the paramagnetic limit and the solution for the function $m(E)$ for both spin directions. (a) and (d) are for $\hbar/\tau_{\rm SO} = 0$; (b) and (e) are for a small spin-orbit coupling $\hbar/\tau_{\rm SO}\Delta = 0.1$; (c) and (f) are for $\hbar/\tau_{\rm SO}\Delta = 0.2$, $\mu_0\mu_B H = \Delta/2$.

From this solution for the density of states, we can predict some of the qualitative changes in the complex conductivity:

We expect a shift of the spectroscopic gap to an energy slightly higher than $2\Delta - 2\mu_0\mu_B H$. An even more interesting effect is the fact that a new transition channel is now possible, where one of the quasiparticles is excited to the "mixed" spin states at low energy. This new channel enhances $\sigma_1$ for low frequencies, thus leading to an increased absorption below the equilibrium gap $2\Delta_0$. A third effect which is expected from this solution of the density of states is a smearing of the peak in the density of spin-up states.

In order to calculate the complex conductivity $\sigma(\omega)$, we will generalize the Skalski results[20] for the case of a more general (magnetic and nonmagnetic) spin-flip scattering in the paramagnetic limit. The most important difference with the Skalski approach is the fact that we now have to solve the Green's functions for both spin directions separately.

We finally obtain

$$\frac{\sigma_1(\omega)}{\sigma_n} = \frac{1}{\hbar\omega}\sum_{s,s'} |A_{ss'}|^2 \times \int_{\Delta-\mu_0\mu_B H-\hbar\omega}^{-\Delta+\mu_0\mu_B H} dE\,[n_s(E)n_{s'}(E+\hbar\omega) + m_s(E)m_{s'}(E+\hbar\omega)] , \tag{31}$$

where

$$n_s(E) = \mathrm{Re}\left[\frac{u_s}{(u_s^2-1)^{1/2}}\right] , \quad m_s(E) = \mathrm{Re}\left[\frac{1}{(u_s^2-1)^{1/2}}\right] , \tag{32}$$

and $u_s$ are the solutions to the coupled equations (30).

The function $n_s(E)$ is again the density of states for quasiparticles with spin $s$, and an even function of $E$. The function $m_s(E)$ is odd with respect to $E$, and has no direct physical meaning.

The solution for $m_\uparrow$ and for $m_\downarrow$ is plotted in Figs. 12(d)–12(f) for the same parameters as in Figs. 12(a)–12(c).

An interesting result is that $m_\uparrow$ is practically zero near $E = \Delta - \mu_0\mu_B H$. This means that the new transition channel in $\sigma_{\uparrow\uparrow}$, where one of the quasiparticles is excited to the mixed spin states, obeys a coherence factor $F \approx 1$, which is more familiar to a case-I perturbation. For comparison, upon evaluating the spin-flip transition rate $\sigma_{\uparrow\downarrow}$ for frequencies near $\hbar\omega \approx 2\Delta - 2\mu_0\mu_B H$, one finds that both terms in the integrand of Eq. (31) have a different sign and approximately cancel each other. That is, it obeys a

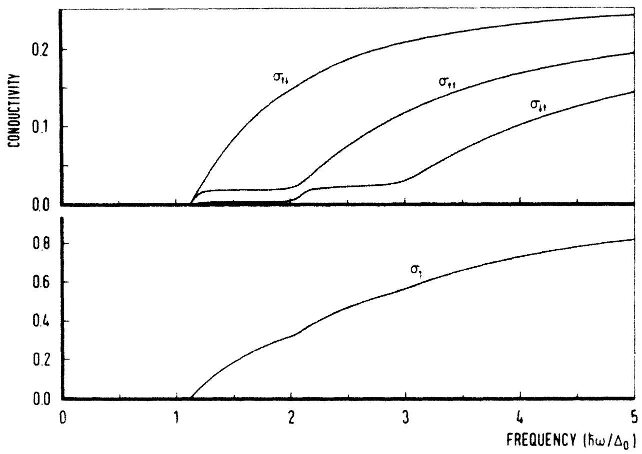


FIG. 13. Real part of the conductivity, calculated according to Eqs. (30)–(32) for a spin-flip probability 0.5 and $\hbar/\tau_{SO}\Delta=0.1$. (a) the contributions $\sigma_{1\uparrow\downarrow}$, $\sigma_{1\uparrow\uparrow}=\sigma_{1\downarrow\downarrow}$, and $\sigma_{1\downarrow\uparrow}$ corresponding to the different channels. (b) The total conductivity $\sigma_1$, which is a summation of the four contributions shown in (a).

typical case-II coherence factor $F\approx 0$ at frequencies near the gap. In Fig. 13 we have calculated the full conductivity $\sigma_1$ according to Eqs. (29)–(31), for the parameters as in Figs. 12(b) and 12(e). We find an almost constant level of $\sigma_{1\uparrow\uparrow}=\sigma_{1\downarrow\downarrow}$ for the transition to the mixed spin state, due to the fact that $F\approx 1$. A similar plateau is also observed for the reverse spin-flip excitation $\sigma_{1\downarrow\uparrow}$. For the total conductivity $\sigma_1$ we find an enhanced value at low frequencies, a slightly increased gap, and a smoothing of the structure

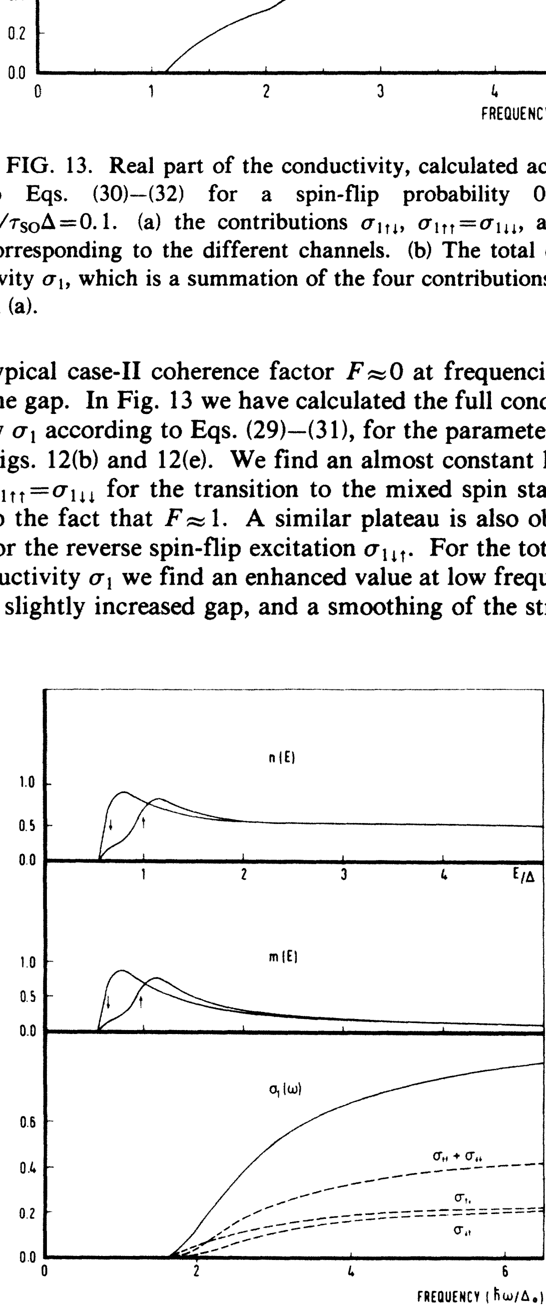


FIG. 14. (a) Density of states for a film with both spin-orbit coupling and spin-flip scattering ($\hbar/\tau_{SO}\Delta=0.1$ and $\hbar/\tau_{SF}\Delta=0.06$, $\mu_0\mu_B H=0.1\Delta$. (b) The function $m(E)$ for both spin directions with the same parameters as in (a). (c) The complex conductivity for this film assuming a spin-flip probability of 0.5.

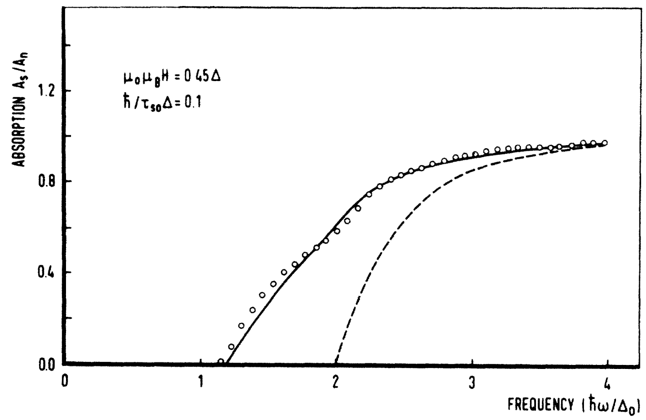


FIG. 15. Experimental result for the absorption of film 6 for $\mu_0 H=2.24$ T and $T/T_c=0.2$ compared with a calculation using the conductivity $\sigma_1$ shown in Fig. 17, assuming a spin-flip probability of 0.5 and a spin-orbit coupling $\hbar/\tau_{SO}\Delta$ of 0.1 and an *ad hoc* value of $\sigma_2=0.7\sigma_2^{MB}$.

near $\hbar\omega=2\Delta$; the structure at $2\Delta+2\mu_0\mu_B H$ has almost disappeared.

The inclusion of (magnetic) spin-flip scattering can be treated in a similar way. For example, in Fig. 14 we have calculated the density of states, the function $m(E)$, and the real part of the conductivity for a film with both spin-orbit and spin-flip scattering ($\hbar/\tau_{SO}\Delta=0.1$ and $\hbar/\tau_{SF}\Delta=0.06$). These values correspond with the experimental parameters for film 4 in a field $H/H_c=0.36$ (Fig. 5). Although it is clear that even in this (pair-breaking) situation we can clearly distinguish spin-dependent properties, the total conductivity does not show a paramagnetic structure and is approximately equal to the result obtained by Skalski.

Let us now turn to a direct comparison of the present theory and experimental results for ultrathin films. In Fig. 15 we have plotted the experimentally observed absorption of film 6 in a field $\mu_0 H=2.24$ T ($\mu_0\mu_B H=0.45\Delta$) together with a theoretical calculation, using $\hbar/\tau_{SO}\Delta=0.1$, $\hbar/\tau_{SF}\Delta=0$, and an electromagnetic spin-flip probability of 0.5. In accordance with Ref. 18, we further assumed an additional electron-phonon coupling which reduces the imaginary part of the conductivity $\sigma_2=0.7\sigma_2^{MB}$.

With these parameters we indeed find good quantitative agreement between theory and experiment. The resolution of the spectrometer used does not allow a more detailed evaluation of the data.

A similar analysis of the absorption spectra at different magnetic field values and for different films confirms the present conclusions of a spin-orbit coupling $0<\hbar/\tau_{SO}\Delta<0.2$.

## VI. ANOMALIES

An exception behavior was observed for film 3, which had a thickness of only 3 nm. The absorption measurements for different field values is depicted in Fig. 16. This film had a significantly higher resistivity ($R_n=2.1$

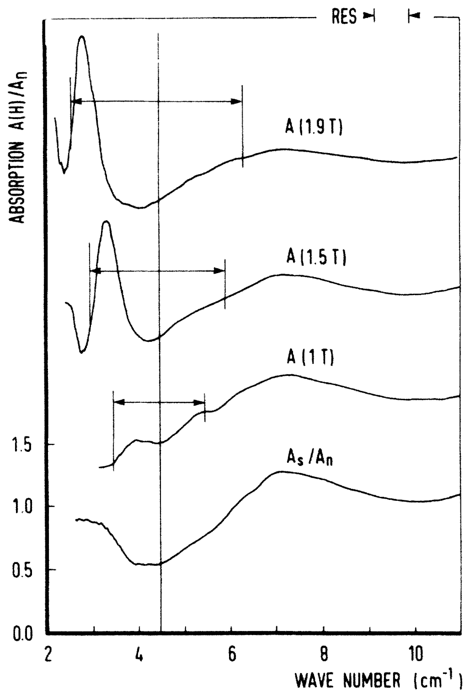


FIG. 16. Absorption of film 3 ($d=3$ nm) as a function of frequency for different values of the parallel magnetic field. The theoretically expected energy gap $2\Delta-2\mu_0\mu_B H$ and of the kinks at $\hbar\omega=2\Delta$ and at $\hbar\omega=2\Delta+2\mu_0\mu_B H$ are indicated.

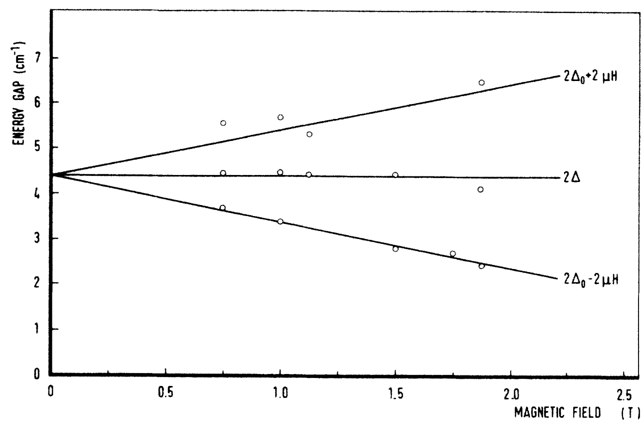


FIG. 17. Spectroscopic gap $\Omega_g$ and position of the steps as a function of the parallel magnetic field for film 3. The solid lines indicate the theoretically expected values given by $\hbar\omega=2\Delta$ and $\hbar\omega=2\Delta\pm2\mu_0\mu_B H$.

k$\Omega$), which indicates a strong granular structure. A problem which complicates the absorption measurements on Si substrates (films 1—3) is the rather high refractive index of $n=3.4$. This leads to an interference pattern with a period of about 8 cm$^{-1}$. However, the interference effects cancel in the ratio of the absorption and transmission, which gives the real part of the conductivity, and we found a good agreement with the Mattis-Bardeen calculations for frequencies above the gap. Due to this interference effect, we were not able to correct the absorption spectra for the background signal, but we clearly observed the field-dependent structure described before. More specifically, we again found the field-dependent shift of the spectroscopic gap (Fig. 17). In this particular case, we also found some structure on the absorption edge shifting upward with increasing field: $\hbar\omega\approx2\Delta+2\mu_0\mu_B H$. A peculiar phenomenon for this film was that for the higher fields of 1.5 and 1.9 T ($H/H_c=0.39$, respectively 0.50), we found that the shoulder shifting to low frequencies developed into a narrow peak (see Fig. 16). The edge of this peak still shifted linearly with the field, according to $\hbar\omega=2\Delta-2\mu_0\mu_B H$, but the absorption maximum increased to about twice the normal-state absorption. This absorption peak was clearly visible in the absorption spectrum before it was normalized by the normal-state absorption. We believe therefore that this anomalous absorption is experimentally significant. This was confirmed by a reference measurement of the absorption at a fixed frequency of 40 GHz, while sweeping the field. We found again near $\mu_0\mu_B H\approx\Delta/2$ an absorption which was considerably higher than the normal-state absorption.

At present we cannot explain the anomalous absorption of this granular film. Although the inclusion of spin-orbit interaction does give a much stronger absorption at frequencies just above the spectroscopic gap, it cannot explain the presence of a pronounced peak. The calculations in Sec. V A, which included the contribution of the quasiparticle scattering term, predict the presence of a peak in the real part of the conductivity when $T\neq0$ and $\hbar\omega\approx2\mu_0\mu_B H$, as is the case in the upper curve of Fig. 16. However, it seems unlikely that this quasiparticle scattering term gives an appreciable absorption at the temperatures presently used ($T/T_c\leq0.3$).

## VII. CONCLUSIONS

We have presented FIR-absorption measurements on thin and ultrathin superconducting Al films in a parallel magnetic field. For films with $d\approx10$ nm we find a shift of the energy gap which is in good agreement with the AG theory of pair-breaking. For ultrathin films we observed a linear shift of the spectroscopic gap according to $\hbar\omega=2\Delta-2\mu_0\mu_B H$, which is attributed to a photon absorption process where an antiparallel Cooper pair is broken into two spin-down quasiparticles. We have developed a theory within the BCS framework which gives the complex conductivity of a superconducting film in the paramagnetic limit and which includes the effect of photon-induced spin-flip processes. The effect of spin-orbit and (magnetic) spin-flip scattering on the complex conductivity is evaluated using a Green's-function formalism. We find good quantitative agreement between the experimentally observed FIR absorption of ultrathin paramagnetically limited Al films and the present theory, assuming that $\hbar/\tau_{SO}\Delta\approx0.1$ and that $\sigma_2$ is reduced because of an enhanced electron-phonon coupling. The anomalous absorption of a granular 3-nm-thick film is not understood.

*Also at Max-Planck-Institut für Festkörperforschung, Hochfeld-Magnetlabor, 25, Avenue des Martyrs, 166 X, F-38042 Grenoble Cedex, France.

[1]J. Bardeen, L. N. Cooper, and J. R. Schrieffer, Phys. Rev. **108**, 1175 (1957).

[2]K. Yosida, Phys. Rev. **110**, 769 (1958).

[3]P. Fulde and R. A. Ferrell, Phys. Rev. **135**, A550 (1964); H. Engler and P. Fulde, Phys. Kondens. Mater. **7**, 150 (1968).

[4]A. M. Clogston, Phys. Rev. Lett. **9**, 266 (1962); B. S. Chandrasekhar, Appl. Phys. Lett. **1**, 7 (1962); G. Sarma, J. Phys. Chem. Solids **24**, 1029 (1963); K. Maki and T. Tsuneto, Prog. Theor. Phys. **31**, 945 (1964).

[5]J. Bardeen and J. R. Schrieffer, in *Low Temperature Physics,* edited by C. J. Gorter (North-Holland, Amsterdam, 1961), Vol. 3, p. 170.

[6]R. H. Hammond and G. M. Kelly, Phys. Rev. Lett. **18**, 156 (1967).

[7]H. L. Fine, M. Lipsicas, and M. Strongin, Phys. Lett. **29A**, 366 (1969).

[8]M. Strongin and O. F. Kammerer, Phys. Rev. Lett. **16**, 456 (1966).

[9]P. M. Tedrow and R. Meservey, Phys. Rev. Lett. **24**, 1004 (1970).

[10]P. M. Tedrow and R. Meservey, Phys. Rev. B **8**, 5098 (1973).

[11]R. Meservey, P. M. Tedrow, and P. Fulde, Phys. Rev. Lett. **25**, 1270 (1970); P. M. Tedrow and R. Meservey, *ibid.* **27**, 919 (1971); R. Meservey and P. M. Tedrow, Phys. Rev. B **11**, 4224 (1975).

[12]P. M. Tedrow and R. Meservey, Phys. Rev. Lett. **26**, 192 (1971); Phys. Lett. **69A**, 285 (1978); P. M. Tedrow, J. S. Moodera, and R. Meservey, Solid State Commun. **44**, 587 (1982); P. M. Tedrow, J. T. Kucera, D. Rainer, and T. P. Orlando, Phys. Rev. Lett. **52**, 1637 (1984).

[13]See, for example, K. E. Gray, in *Nonequilibrium Superconductivity, Phonons and Kapitza Boundaries,* edited by K. E. Gray (Plenum, New York, 1981), Chap. 5, p. 131.

[14]A. A. Abrikosov and L. P. Gor'kov, Zh. Eksp. Teor. Fiz. **39**, 1781 (1960) [Sov. Phys.—JETP **12**, 1243 (1961)].

[15]D. M. Ginsberg and M. Tinkham, Phys. Rev. **118**, 990 (1960).

[16]L. H. Palmer and M. Tinkham, Phys. Rev. **165**, 588 (1968).

[17]W. S. Martin and M. Tinkham, Phys. Rev. **167**, 421 (1968).

[18]P. J. M. van Bentum and P. Wyder, Physica **138B**, 23 (1986).

[19]K. Maki and P. Fulde, Phys. Rev. **140**, A1586 (1965).

[20]S. Skalski, O. Betbeder-Matibet, and P. R. Weiss, Phys. Rev. **136**, 1500 (1964).

[21]J. L. Levine, Phys. Rev. **155**, 373 (1967).

[22]G. J. Dick and F. Reif, Phys. Rev. **181**, 774 (1968).

[23]B. T. Matthias, H. Suhl, and E. Corenzwit, Phys. Rev. Lett. **1**, 93 (1960).

[24]J. W. Hendriks, H. R. Ott, J. H. M. Stoelinga, and P. Wyder, Solid State Commun. **21**, 555 (1977); C. G. C. M. de Kort, J. H. M. Stoelinga, and P. Wyder, Physica **110B**, 1 (1980).

[25]D. C. Mattis and J. Bardeen, Phys. Rev. **111**, 412 (1958).

[26]R. L. de Kronig, J. Opt. Soc. Am. **12**, 547 (1926); H. A. Kramers, Atti. Congr. Fis. Como **2**, 545 (1927); also see M. Tinkham, in *Low Temperature Physics,* edited by C. de Witt B. Dreyfus, and P. G. de Gennes (Gordon and Breach, New York, 1962).

[27]M. Tinkham and R. A. Ferrell, Phys. Rev. Lett. **2**, 331 (1968).

[28]P. Fulde, Adv. Phys. **22**, 667 (1973).

[29]H. Engler and P. Fulde, Z. Phys. **247**, 1 (1971).

[30]A. A. Abrikosov and L. P. Gor'kov, Zh. Eksp. Teor. Fiz. **35**, 1558 (1958) [Sov. Phys.—JETP **8**, 1090 (1959)].

[31]Y. Nambu, Phys. Rev. **117**, 648 (1960).

[32]J. Keller and R. Benda, J. Low Temp. Phys. **2**, 144 (1970).

[33]R. C. Bruno and B. B. Schwartz, Phys. Rev. B **8**, 3161 (1973).